Jurnal Perkeretaapian Indonesia (Indonesian Railway Journal) Vol.8 No. 2 Oktober, 2024
p-ISSN 2550-1127/e-ISSN 2656-8780

Evaluation of ultrasonic non-destructive inspection methods for structural integrity assessment of freight train axles

Irwan Maulana[1], M. Agus Kariem[2], R. Dadan Ramdan[3]
Program Studi Teknik Mesin Institut Teknologi Bandung, Labtek PPTI Jalan Ganesa No.10, Bandung 40132, Jawa Barat, Indonesia[1].
Fakultas Teknik Mesin dan Dirgantara, Institut Teknologi Bandung, Jalan Ganesa No 10, Bandung 40132, Jawa Barat, Indonesia[2,3]
*E-mail address: 23122032@mahasiswa.itb.ac.id

ABSTRAK

Penilaian integritas struktural bertujuan untuk memastikan kepatuhan terhadap standar keselamatan, kekuatan, dan kinerja yang ditentukan. Penilaian ini beroperasi berdasarkan prinsip toleransi kerusakan, memastikan bahwa kegagalan dapat dihindari selama struktur tetap berada dalam kapasitas penahan bebannya, meskipun terdapat cacat atau retakan, sesuai dengan kriteria mekanika retakan. Dengan menggabungkan probabilitas deteksi dari prosedur *non-destructive inspections* (NDI), konsep toleransi kerusakan memastikan keamanan gandar selama operasi. Studi ini menguji sensitivitas metode NDI dalam mendeteksi kerusakan dan membandingkan hasilnya dengan kriteria penilaian integritas struktural yang diuraikan dalam BS 7910. Untuk mendapatkan hasil analisis yang akurat, penelitian ini menggunakan simulasi numerik dengan metode elemen hingga menggunakan perangkat lunak ANSYS. Hasilnya menunjukkan bahwa ukuran cacat kritis adalah 80 mm sesuai dengan kriteria yang ditentukan dalam BS7910. Selain itu, analisis sensitivitas NDI menunjukkan bahwa NDI dapat mendeteksi ukuran cacat terkecil sebesar 4 mm, meskipun dengan pulsa indikasi yang sangat rendah, dan dapat mendeteksi cacat dengan pulsa deteksi yang cukup baik pada ukuran cacat 10 mm.

Kata Kunci: Penilaian integritas struktur, Inspeksi ultrasonic tak-merusak, Analisis toleransi kerusakan

ABSTRACT

Structural integrity assessment aims to ensure compliance with specified safety, strength, and performance standards. It operates on the principle of damage tolerance, ensuring that failure is avoided as long as the structure remains within its load-bearing capacity, despite the presence of defects or cracks, according to fracture mechanics criteria. By combining the probability of detection from the NDI procedure, the damage tolerance concept ensures the safety of the axle during operation. This study examines the sensitivity of the NDI method in detecting damage and compares its results with the structural integrity assessment criteria outlined in BS 7910. To obtain accurate analysis results, this study utilized numerical simulations with the finite element method using ANSYS software. The results indicated that the critical defect size is 80 mm according to the criteria specified in BS7910. In addition, the sensitivity analysis of NDI showed that NDI can detect the smallest defect size of 4 mm, albeit with a very low indication pulse, and can detect defects with a sufficiently good detection pulse at a defect size of 10 mm.

Keywords: Structural integrity assessment, Ultrasonic non-destructive inspections, Damage tolerance analysis

1 INTRODUCTION

Fundamentally, the axle design concept aims to prevent crack initiation. However, there is still a possibility of cracks occurring due to operation within service life [1]. Common damages found in railway axles include defects from foreign object impacts, scratches, and corrosion [2]. These defects often serve as the root cause of structural failures [3–5]. At certain sizes, defects can become the starting point for fatigue crack initiation [6], where crack propagation occurs gradually due to repeated loading cycles. If fatigue cracks go undetected, they will continue to grow until reaching critical sizes, potentially leading to failure.

1.1 A recent failure cases

In September 2016, a freight train with 50 wagons derailed between Negararatu Station and Ketapang Station, causing seven wagons to derail and one wagon to suffer a broken axle. In April 2018, a flat car train went off the tracks at Karangsari Station, disrupting regular train services and causing significant delays. The investigation found that one wagon had a broken axle. In 2021, a coal freight train derailed between Giham and Belambangan umpu, overturning and revealing a broken axle.

Crack initiation is likely to begin from corrosion pits in areas where the coating layer has detached from the surface. These corrosion pits elevate local stresses on the axle surface, initiating crack formation. Subsequently, these cracks propagate, eventually leading to the axle breaking into two pieces. Köhler reported in his research that approximately 85% of axle failures in freight trains are due to corrosion damaging the axle surface [7].

Figure 1 The fracture of the railway axle [8]

Non-destructive inspections (NDI) using ultrasonic methods are performed periodically during the railway's service life. However, despite this fact, the axle cracked in the middle span area (see

Figure 2), a location quite distant from the position of the ultrasonic transducer during inspection. This condition is known as the far-end scanning condition in ultrasonic testing. Refer to section 3 for a more detailed discussion.

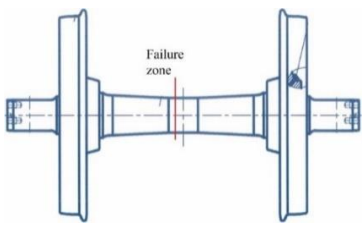

Figure 2 The freight train wheelset with the highlight of the failure zone.

1.2 Non-destructive inspection

To ensure safety during service, periodic NDI is conducted on the axles. NDI must be able to identify defects at the smallest size before they reach critical dimensions that could lead to catastrophic failure [9]. The sensitivity of NDI to detect defects as required in the inspection documents is closely related to the safety integrity of the structural component [10]. Generally, railway axle inspections utilize ultrasonic testing methods. The use of ultrasonic testing is chosen for its speed and efficiency, thereby minimizing significant downtimes for railway operations.

1.3 Structural integrity assessment

The structural integrity assessment aims to ensure that the structure meets specified safety, strength, and performance requirements. This assessment procedure has long been developed in Europe involving seventeen organizations from nine European countries [11]. In assessing the structural integrity of railway axles, this assessment is based on the damage tolerance concepts, wherein failure can be avoided as long as the structure is not subjected to loads exceeding its maximum capacity due to the presence of defects or cracks, using fracture mechanics criteria [11,12]. This evaluation concept is heavily influenced by the structure, size, and shape of cracks, material tensile properties, and loading conditions [14]. Guidance for assessment methods can follow the BS7910 document [15].

2 METHOD

This study employs two approaches: firstly, conducting experiments using an ultrasonic flaw detector to identify the smallest detectable defect size, and secondly, analyzing based on the BS7910 standard to ascertain critical defect sizes. To enhance the accuracy of the analysis, the study will also involve simulations using finite element methods. The overall research workflow is depicted in Figure 3.

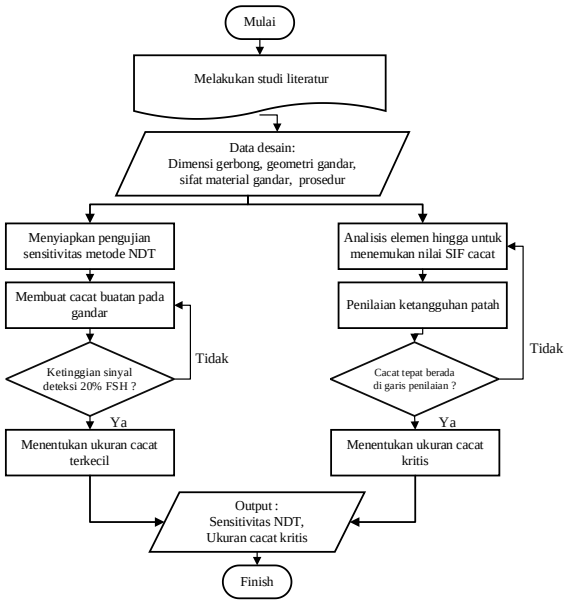

Figure 3 Research methodology

3 ULTRASONIC NON-DESTRUCTIVE INSPECTION EVALUATION

The ultrasonic NDI exhibits different probability of detection (POD) characteristics between near-end and far-end scanning conditions. Near-end scanning conditions yield better results in detecting shallow crack depths. The discussion on the characteristics of POD data between near-end and far-end ultrasonic inspection on railway axles can be found in the literature [16].

In this study, an evaluation of the sensitivity of ultrasonic NDI methods was conducted using conventional transducers on freight train axles. The assessment was performed under far-end scanning conditions, where the transducer was positioned far from the inspected area, allowing for the detection of defects in the mid-span or near the mid-span of the axle. This method tests the ability of conventional transducers to effectively generate and receive ultrasonic waves.

Artificial defects are placed at the mid-span of the axle with varying depths, as illustrated in Figure 4. The experiment was performed using a 25.4mm transducer at 2 MHz frequency, with a typical amplification of 60-80 dB, depending on the crack depth being inspected. The experiment proceeds with a gradual increase in defect depth, starting from 2mm and continuing until a pulse height of 20% Full-Scale Height (FSH) or higher is detected [17]. Under these conditions, the presence of defects can be readily identified. The experimental findings are given in detail in Figure 5.

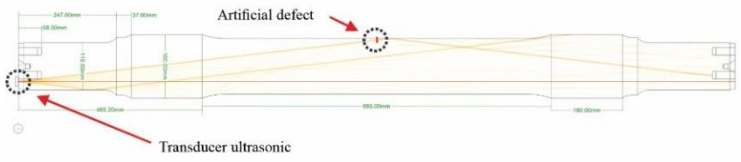

a)

b)

Figure 4 The experimental setup a) defect location and probe position b) artificial defect.

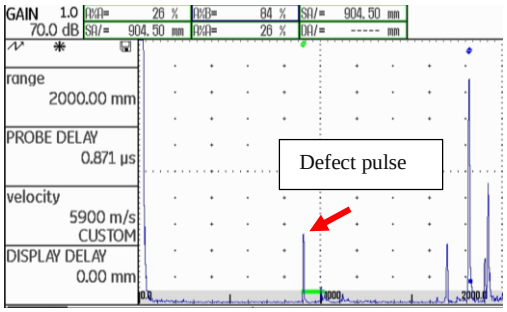

a)

Defect depth (mm)	% FSH
2	0
3	0
4	2
5	2
6	3
7	4
8	7
9	9
10	10
11	16
12	17
13	26

b)

Figure 5 The pulse representation against defect depth a) A-scan display, b) the variation of pulse height and defect depth.

4 SIMULATION MODEL

The vertical load P, resulting from the train weight, is transmitted to the wheelset through the journal area. This load distribution induces bending moments in the axle. Figure 6 depicts the load distribution scheme of the wheelset.

Numerical methods are commonly employed to analyze complex loads, including railway axle load analysis, as found in the literature [18]–[21]. The analysis is conducted by simplifying the wheelset as shown in Figure 6b, to streamline computational calculations without compromising the overall accuracy of the analysis results. This simplification is known as the symmetry technique in FEM analysis [22].

4.1 Loading conditions

The axle is subjected to a vertical force of 17375 kg distributed across both journals at the ends of the axle, representing the total load of the train at 69500 kg, taking into account the dynamic factor and lateral force due to the operational speed of the train as stated in the literature [23]. The analysis utilizes ANSYS software with tetrahedral elements, and convergence testing is conducted by progressively refining the mesh in simulations. The results of the convergence test are presented in Figure 7.

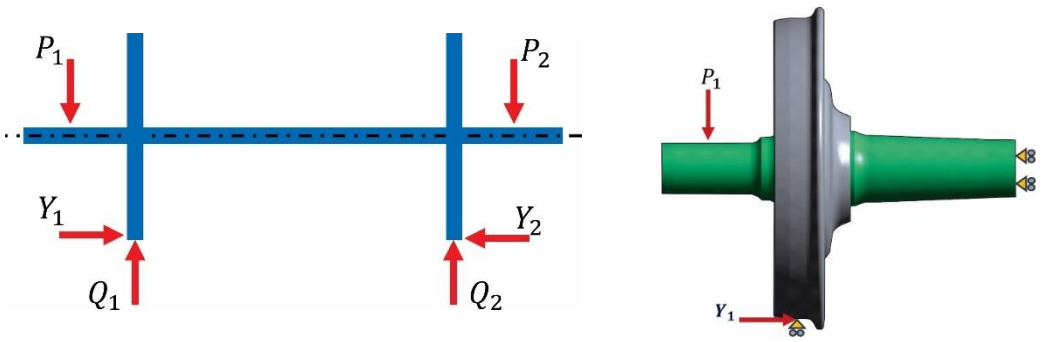

a) b)

Figure 6 The load distribution a) scheme on the wheelset b) Simplifying FE model of a freight train wheelset.

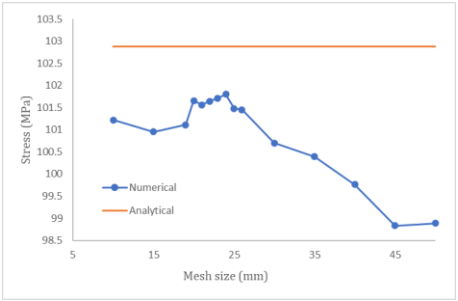

Figure 7 Convergence and validation model FE with analytical solution.

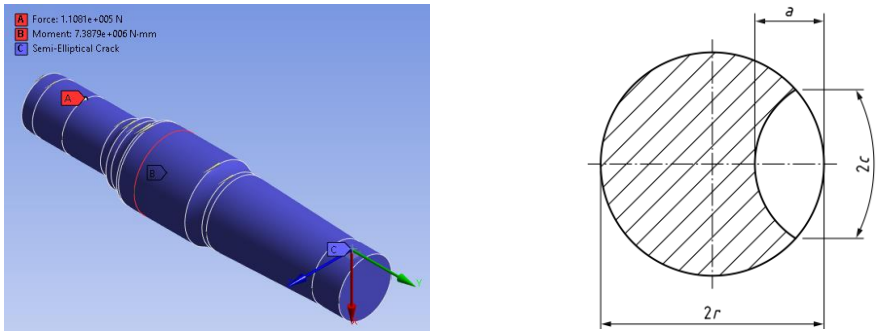

a) b)

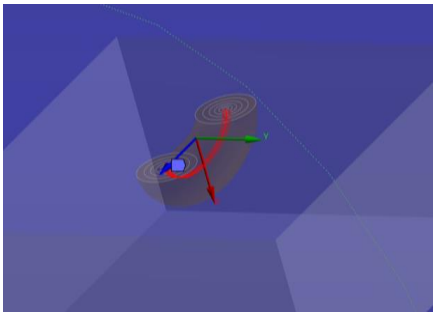

c)

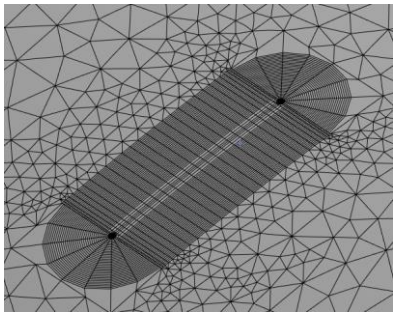

d)

Figure 8 The setup of the finite element model, a) the global geometry, b) the geometry of the semi-elliptical crack, c) the application of the crack in the sub-model, and d) the refinement of the mesh around the crack.

4.2 Crack configuration

A semi-elliptical defect is introduced at the same location where the failure zone occurred on the axle. The dimensions of the defect adhere to the procedures outlined in BS7910, with the depth of the crack represented by "a", axle diameter 2r, and the length of the crack represented by "2C". The implementation of the simulation model is depicted in Figure 8.

5 THE STRUCTURAL INTEGRITY ASSESSMENT PROCEDURE

This assessment aims to evaluate the structural capacity to withstand fractures caused by defects or cracks in the structure. The analysis commences with identifying the axle material characteristics, determining the Stress Intensity Factor (SIF), and establishing an acceptable region based on BS7910 guidelines. Subsequently, crack ratio and load ratio calculations are performed. The outcomes are depicted in an assessment point diagram based on the crack ratio and load ratio. Thus, assessment points can be positioned within a critical region where defects would reach a critical size that could lead to the final failure of the axle.

5.1 Material properties

The freight train axles are manufactured from medium carbon steel by the AAR M101 Grade F [24]. The modulus of elasticity E is set at 200 GPa [18], and tensile tests have been carried out to determine the mechanical properties of the axle material, ensuring its compliance with AAR requirements and as input parameters for subsequent analysis stages. The required chemical composition and mechanical properties outlined in the AAR standard, together with the test results obtained from the axles, are shown in Table 1 and Table 2.

Table 1 Chemical composition for AAR M101 Grade F [24]

	C	Mn	P	S	Si
AAR standard	0.45-0.59	0.6-0.9	Max. 0.045	Max. 0.05	min. 0.15
Freight train axles	0.512	0.771	0.013	0.002	0.279

Table 2 Mechanical properties for AAR M101 Grade F [24]

	σ_Y (MPa)	σ_{UTS} (MPa)	A (%)	Z (%)
AAR standard	Min. 345	Min. 607	Min. 22	Min. 37
Freight train axles	396	721	22	49

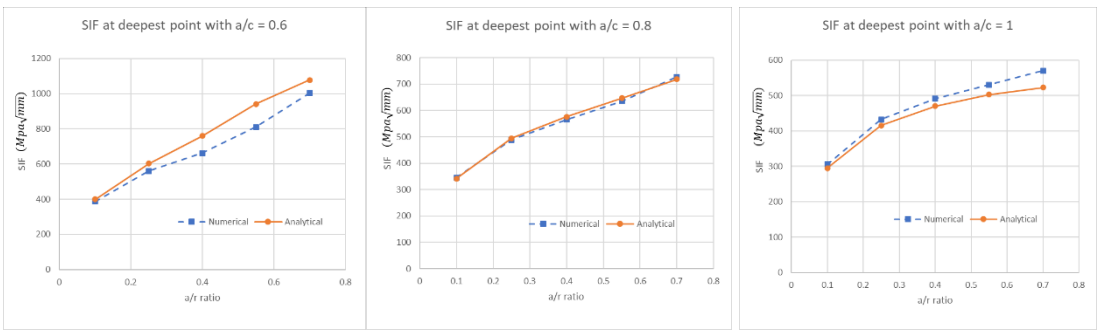

a) SIF comparison at the deepest point

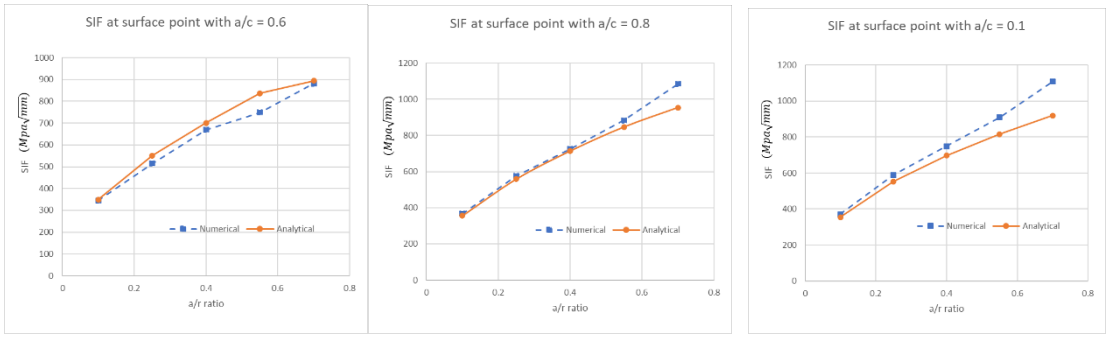

b) SIF comparison at the surface point

Figure 9 SIF comparison between an analytical solution with FE result

5.2 Determine the stress intensity factor (SIF) solution

Stress Intensity Factor (SIF) is a critical input parameter in structural integrity analysis, and its solution can be obtained through Finite Element Analysis (FEA) or analytical methods extensively discussed in relevant literature [24,25]. The SIF solution in this study follows the equations given in document BS7910 as follows:

$$K_I = (Y\sigma)\sqrt{\pi\alpha} \quad (1)$$

Where Y is the stress intensity factor correction, determined based on the structure's geometry and defect configuration.

The SIF analysis is conducted separately between the deepest point of the crack and the point on the crack surface. This division is essential to consider the distinct stress conditions encountered at these two locations. Figure 9 illustrates the SIF analysis results at both points using Finite Element (FE) and analytical solutions.

5.3 Estimation of fracture toughness

Fracture toughness is a material property that quantifies the ability of a material to resist fractures. In this study, the fracture toughness is estimated by correlating it with Charpy V-notch impact test data using the following equation:

$$K_{mat} = [(12\sqrt{C_v} - 20)(25/B)^{0.25}] + 20 \quad (2)$$

5.4 Failure assessment diagram (FAD)

The FAD approach is based on the concept of elastic-plastic behavior, although its application is simplified by considering only elastic parameters. There are 3 assessment levels in the BS7910 guideline, and the choice of level depends on the materials involved, the available input data, and the desired level of conservatism. Level 1 is the most conservative among the 3 levels, while level 2 represents the normal assessment route. For safety purposes, this study utilizes a Level 1 assessment line. The assessment line is established by the following equation:

$$f(L_r) = \left(1 + \frac{1}{2}L_r^2\right)^{-0.5}[0.3 + 0.7exp(-\mu L_r^6)]$$

$$\text{for } L_r \leq 1 \quad (3)$$

$$K_r = f(L_r) = f(1)\, L_r^{(N-1)/(2N)}$$

$$\text{for } 1 \leq L_r \leq L_{r,maks} \quad (4)$$

$$f(L_r) = 0 \text{ for } L_r \geq L_{r,maks} \quad (5)$$

and the cutoff point of the curve is determined by the equation:

$$L_{r,max} = \frac{\sigma_Y + \sigma_u}{2\sigma_Y} \quad (6)$$

In the FAD assessment, the comparison between the driving force of the crack tip (K_I) and the fracture toughness of the material (K_{mat}), as well as the plastic collapse load analysis, is performed simultaneously. The vertical axis on the FAD represents the ratio of the stress intensity factor to the fracture toughness of the material, while the horizontal axis represents the ratio of stress to yield stress. The fracture ratio K_r and load ratio L_r are determined using the equations (7) and (8).

$$K_r = \frac{K_I}{K_{mat}} \quad (7)$$

$$\text{and} \quad L_r = \frac{\sigma_{reff}}{\sigma_Y} \quad (8)$$

If the assessment point lies within the area bounded by the assessment line, it indicates that the flaw will not lead to fracture. Fracture occurs when the assessment point equals or is outside the assessment line. This means that the flaw has reached a critical dimension, reducing the ability of the structure to withstand the

applied load.**Error! Reference source not found.**

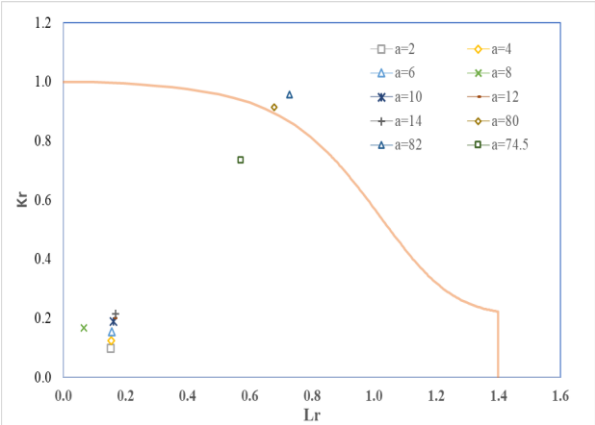

*Figure 10 Failure assessment diagram (FAD) for the small cracks that ultrasonic NDI can detect and critical size crack.***Error! Reference source not found.**Figure 10 illustrates the assessment points of artificial defects utilized in evaluating the sensitivity of NDI. The assessment results are compared with their positions relative to the assessment line, yielding unity check (UC) values presented in Table 3. These values represent the acceptability level of defects in the structure. The higher value, the more hazardous it is to the structural integrity.

The critical defect size analysis is based on three different points, each representing defects at depths of 74.5 mm, 82 mm, and 80 mm. At a defect depth of 80 mm, the assessment point aligns precisely with the FAD assessment line, indicating that the defect size approaches the critical point. However, at greater defect depths, the assessment point shifts further away from the FAD assessment line, indicating a higher potential for structural failure associated with these defects.

Table 3 unity check values

Defect depth (a)	Nilai SIF $Mpa\sqrt{mm}$	Lr	Kr	UC
2	223	0.1527	0.0980	0.157
4	280	0.1545	0.1231	0.173
6	350	0.1567	0.1538	0.192
8	383	0.0671	0.1683	0.172
10	431	0.1620	0.1894	0.220
12	452	0.1651	0.1986	0.229
14	489	0.1686	0.2149	0.243

The failure of freight train axles has also been documented in the literature [6]. The axles made from solid bars, experienced fractures at the mid-span of the axle. At the fracture site, the diameter of the axle measures 171mm, with a critical flaw size of about 120mm from the outer surface. The fracture pattern is shown in Figure 11a. Furthermore, FE analysis in this study, depicted in Figure 11b, identifies a critical defect depth of 80mm, with the axle diameter at 149mm.

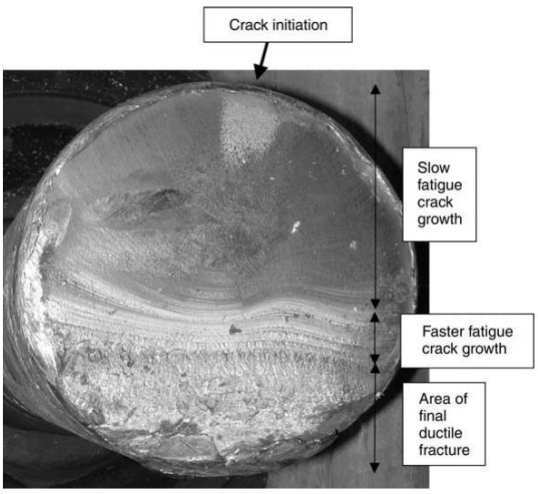

a)

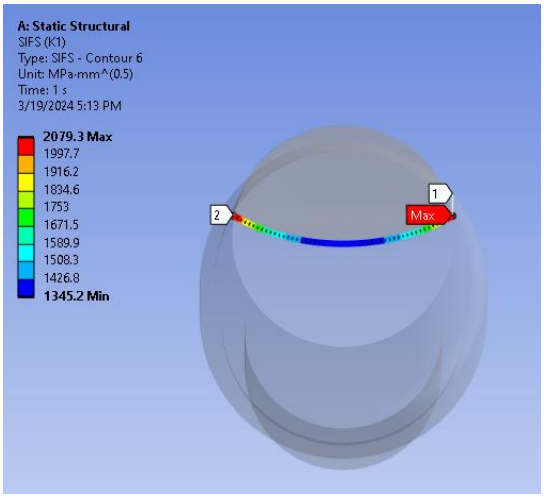

b)

Figure 11 Critical defect on solid axles: a) The fracture surface of solid axle reported in the literature [6] compared to b) FE analysis results.

6 Concluding remarks

The study investigated the sensitivity of ultrasonic NDI methods for inspecting solid railway axles using far-scan conditions. Structural integrity assessment was conducted through finite element analysis to identify critical defect sizes potentially leading to axle failure, following the BS7910 guidelines commonly adopted across industries. The NDI sensitivity tests yielded the following findings:

- The ultrasonic NDI method can detect the smallest defects with a depth of 4 mm. However, at this depth, the detection probability was low, with an indication pulse on the screen of only 2% FSH.
- Detection performance was reasonably good for surface defects with a depth of 10mm, with a pulse height of 10% FSH, showing slightly improved detection probability at this level.

The assessment based on numerical simulations indicates that the critical defect size, capable of causing failure, is reached when the defect extends to a depth of 80mm from the surface. This is indicated by the defect assessment point precisely aligning with the assessment line on the FAD curve. Comparing the results of numerical simulations with the minimum defect size that can be effectively detected using Non-Destructive Inspection (NDI), which is 10 mm, reveals a significant difference. The critical defect size is much larger than the minimum detectable defect size. This suggests that the NDI method used is capable of identifying defects before axle failure occurs. However, to ensure timely defect detection, it is crucial to consider crack propagation from the detection size to the critical size. This consideration aids in determining the appropriate intervals for inspection, ensuring that defects are identified before they cause failure.

Reference

[1] M. Maglio *et al.*, "Railway wheel tread damage and axle bending stress – Instrumented wheelset measurements and numerical simulations," *Int. J. Rail Transp.*, vol. 10, no. 3, pp. 275–297, May 2022, doi: 10.1080/23248378.2021.1932621.

[2] J.-W. Gao, X. Dai, S.-P. Zhu, J.-W. Zhao, J. A. F. O. Correia, and Q. Wang, "Failure causes and hardening techniques of railway axles – A review from the perspective of structural integrity," *Eng. Fail. Anal.*, vol. 141, p. 106656, Nov. 2022, doi: 10.1016/j.engfailanal.2022.106656.

[3] U. Zerbst, M. Madia, C. Klinger, D. Bettge, and Y. Murakami, "Defects as a root cause of fatigue failure of metallic components. I: Basic aspects," *Eng. Fail. Anal.*, vol. 97, pp. 777–792, 2019, doi: 10.1016/j.engfailanal.2019.01.055.

[4] U. Zerbst, M. Madia, C. Klinger, D. Bettge, and Y. Murakami, "Defects as a root cause of fatigue failure of metallic components. II: Non-metallic inclusions," *Eng. Fail. Anal.*, vol. 98, pp. 228–239, Apr. 2019, doi: 10.1016/j.engfailanal.2019.01.054.

[5] U. Zerbst, M. Madia, C. Klinger, D. Bettge, and Y. Murakami, "Defects as a root cause of fatigue failure of metallic components. III: Cavities, dents, corrosion pits, scratches," *Eng. Fail. Anal.*, vol. 97, pp. 759–776, 2019, doi: 10.1016/j.engfailanal.2019.01.034.

[6] D. S. Hoddinott, "Railway axle failure investigations and fatigue crack growth monitoring of an axle," *Proc. Inst. Mech. Eng. Part F J. Rail Rapid Transit*, vol. 218, no. 4, pp. 283–292, Jul. 2004, doi: 10.1243/0954409043125897.

[7] U. Zerbst, C. Klinger, and D. Klingbeil, "Structural assessment of railway axles - A critical review," *Eng. Fail. Anal.*, vol. 35, pp. 54–65, 2013, doi: 10.1016/j.engfailanal.2012.11.007.

[8] KNKT, "Laporan Investigasi Kecelakaan Perkeretaapian-Anjlokan Ka 3015 Babaranjang Isi Di Km 119 + 9/0 Petak Jalan Antara St. Negararatu – St.Ketapang," 2017.

[9] A. S. Watson and K. Timmis, "A method of estimating railway axle stress spectra," *Eng. Fract. Mech.*, vol. 78, no. 5, pp. 836–847, 2011, doi: 10.1016/j.engfracmech.2009.12.001.

[10] M. Carboni and S. Cantini, "Advanced ultrasonic 'Probability of Detection' curves for designing in-service inspection intervals," *Int. J. Fatigue*, vol. 86, pp. 77–87, May 2016, doi: 10.1016/j.ijfatigue.2015.07.018.

[11] S. Webster and A. Bannister, "Structural integrity assessment procedure for Europe – of the SINTAP programme overview," *Eng. Fract. Mech.*, vol. 67, no. 6, pp. 481–514, Dec.

2000, doi: 10.1016/S0013-7944(00)00070-9.

[12] U. Zerbst, K. Mädler, and H. Hintze, "Fracture mechanics in railway applications - An overview," *Eng. Fract. Mech.*, vol. 72, no. 2, pp. 163–194, 2005, doi: 10.1016/j.engfracmech.2003.11.010.

[13] M. Luke, I. Varfolomeev, K. Lütkepohl, and A. Esderts, "Fracture mechanics assessment of railway axles: Experimental characterization and computation," *Eng. Fail. Anal.*, vol. 17, no. 3, pp. 617–623, 2010, doi: 10.1016/j.engfailanal.2009.04.008.

[14] U. Zerbst, M. Schödel, and H. T. Beier, "Parameters affecting the damage tolerance behaviour of railway axles," *Eng. Fract. Mech.*, vol. 78, no. 5, pp. 793–809, 2011, doi: 10.1016/j.engfracmech.2010.03.013.

[15] The British Standards Institution, "BS7910:2013+A1:2015 Guide to Methode for Assesing the Acceptability of flaws in Metalic Structure." The British Standards Institution, London, 2015.

[16] M. Carboni and S. Beretta, "Effect of probability of detection upon the definition of inspection intervals for railway axles," *Proc. Inst. Mech. Eng. Part F J. Rail Rapid Transit*, vol. 221, no. 3, pp. 409–417, May 2007, doi: 10.1243/09544097JRRT132.

[17] Association of American railroads, "Manual of standards and recommended practices section G-II." 2010.

[18] E. M. Mueller and X. Liu, "Failure Analysis and Finite Element Modelling of a Rail Axle Fatigue Fracture," *Int. J. Railw. Technol.*, vol. 7, no. 1, pp. 45–63, Apr. 2018, doi: 10.4203/ijrt.7.1.3.

[19] Z. Odanovic, M. Ristivojevic, and V. Milosevic-Mitic, "Investigation into the causes of fracture in railway freight car axle," *Eng. Fail. Anal.*, vol. 55, pp. 169–181, 2015, doi: 10.1016/j.engfailanal.2015.05.011.

[20] V. Giannella, R. Sepe, A. Borrelli, G. De Michele, and E. Armentani, "Numerical investigation on the fracture failure of a railway axle," *Eng. Fail. Anal.*, vol. 129, 2021, doi: 10.1016/j.engfailanal.2021.105680.

[21] D. Ji, J. Zhang, K. Yi, Y. Huang, Q. Lu, and H. Zhang, "Surface crack growth simulation and residual life assessment of high-speed train axles based on extended finite element method," *Eng. Fail. Anal.*, vol. 134, p. 106043, Apr. 2022, doi: 10.1016/j.engfailanal.2022.106043.

[22] D. L. Logan, *A first course in the finite element method*, 4th ed. 2007. doi: 10.1016/0168-874x(87)90008-4.

[23] T. Makino, T. Kato, and K. Hirakawa, "Review of the fatigue damage tolerance of high-speed railway axles in Japan," *Eng. Fract. Mech.*, vol. 78, no. 5, pp. 810–825, 2011, doi: 10.1016/j.engfracmech.2009.12.013.

[24] Association of American railroads, "Manual of standards and recommended practices wheel and axle section G." 2009.

[25] A. Pourheidar, S. Beretta, D. Ragazzi, and C. Baykara, "Comparison of SIF solutions for cracks under rotating bending and their impact upon propagation lifetime of railway axles," *Procedia Struct. Integr.*, vol. 8, pp. 610–617, 2018, doi: 10.1016/j.prostr.2017.12.060.

[26] M. Madia, S. Beretta, M. Schödel, U. Zerbst, M. Luke, and I. Varfolomeev, "Stress intensity factor solutions for cracks in railway axles," *Eng. Fract. Mech.*, vol. 78, no. 5, pp. 764–792, 2011, doi: 10.1016/j.engfracmech.2010.03.019.